



Band gap engineering, band edge emission, and p-type conductivity in wide-gap $\text{LaCuO}_5\text{S}_1\text{xSex}$ oxychalcogenides

著者	Ueda Kazushige, Hosono Hideo
journal or publication title	Journal of Applied Physics
volume	91
number	7
page range	4768-4770
year	2002-04-01
URL	http://hdl.handle.net/10228/572

doi: 10.1063/1.1456240

COMMUNICATIONS

Band gap engineering, band edge emission, and p -type conductivity in wide-gap $\text{LaCuOS}_{1-x}\text{Se}_x$ oxychalcogenidesKazushige Ueda^{a)} and Hideo Hosono*Materials and Structures Laboratory, Tokyo Institute of Technology, 4259 Nagatsuta, Midori, Yokohama 226-8503, Japan*

(Received 18 October 2001; accepted for publication 10 January 2002)

The preparation of $\text{LaCuOS}_{1-x}\text{Se}_x$ solid solutions ($x=0.0, 0.25, 0.5, 0.75,$ and 1.0) was attempted to control their energy gap and band edge emission energy. X-ray diffraction analysis revealed that the lattice constant of $\text{LaCuOS}_{1-x}\text{Se}_x$ increased linearly with increasing x , indicating the formation of a complete solid solution in the LaCuOS – LaCuOSe system. The energy gap estimated from the diffuse reflectance spectra varied continuously from ~ 3.1 eV for $x=0$ to ~ 2.8 eV for $x=1$. The sharp emission near the absorption edge was observed in all samples at room temperature under ultraviolet light irradiation. p -type electrical conduction in these materials was confirmed by Seebeck measurements, and the conductivity was enhanced by substitution of Sr for La. These results demonstrated that the formation of the solid solutions enabled band gap engineering in $\text{LaCuOS}_{1-x}\text{Se}_x$ oxychalcogenides keeping their band edge emission feature and p -type conductivity. © 2002 American Institute of Physics. [DOI: 10.1063/1.1456240]

Electrical and optical properties of various III–V and II–VI compound semiconductors have been widely examined in order to apply them to optoelectronic devices. In particular, wide-gap semiconductors have recently attracted much attention for their applications to light-emitting devices (LEDs) operating at short wavelengths,^{1–3} full-color LEDs,^{4,5} or white-color LEDs.^{6,7} In these applications, band gap engineering of the wide-gap semiconductors is indispensable to fabricate a double heterostructure, to control the energy gap for red–green–blue colors, and to adjust the band gap to the excitation energy for phosphorous materials. Preparation of mixed crystals is usually used as a technique for the band gap engineering of most III–V and II–VI compound semiconductors.

LaCuOS was recently found as a transparent semiconductor, which shows p -type electrical conductivity controllable by acceptor doping and an excitonic emission under ultraviolet (UV) irradiation at room temperature.^{8,9} This material has a layered structure with tetragonal symmetry (space group: $P4/nmm$),¹⁰ in which LaO and CuS layers are alternately stacked along the c axis (Fig. 1). The examination of the electronic structure of LaCuOS (Ref. 11) revealed that the conduction band and valence band are primarily composed of a Cu $4s$ band and Cu $3d$ –S $3p$ hybridized band, respectively. It is, therefore, essential to modulate these Cu and S bands for the control of the energy gap and excitonic emission energy in LaCuOS .

In the survey of the crystal structure of oxychalcogenide-related materials, we knew that the crystal structure of LaCu

OSe reported by Zhu *et al.* is the same as that of LaCuOS .¹² Since only chalcogen ions differ between these materials, the electronic structure of LaCuOSe is expected to be similar to that of LaCuOS . Therefore, it is anticipated that LaCuOSe shows electrical and optical properties similar to those of LaCuOS . Taking into account the electronic structure of LaCuOS , the valence band of LaCuOSe is considered to consist of a Cu $3d$ –Se $4p$ hybridized band. If a complete solid solution forms between LaCuOS and LaCuOSe , the Cu $3d$, S $3p$, and Se $4p$ bands will be hybridized well in the valence band. Namely, the formation of the solid solution will give a modulation in the valence band and enable the band gap engineering of $\text{LaCuOS}_{1-x}\text{Se}_x$.

In this study, we attempted to prepare the solid solutions of $\text{LaCuOS}_{1-x}\text{Se}_x$ ($x=0, 0.25, 0.5, 0.75$ and 1.0) to control their energy gap, and investigated their electrical and optical properties. In particular, the variation of energy gap and luminescent properties in the solid solutions was examined as well as their electrical transport properties.

LaCuOS was synthesized in evacuated silica tubes as reported previously.⁷ LaCuOSe was also prepared by solid-state reactions in evacuated silica tubes. The precursor of La_2Se_3 was first prepared by heating the mixed powder of La metal and Se at 300°C for 6 h. A stoichiometric amount of La_2O_3 , La_2Se_3 precursor, Cu metal, and Se was mixed, and LaCuOSe was obtained by heating the mixed powder at 600°C for 6 h. $\text{LaCuOS}_{1-x}\text{Se}_x$ ($x=0.25, 0.5,$ and 0.75) was prepared by heating the mixed powder of LaCuOS and LaCuOSe at 800°C for 6 h. The powder of each sample was isostatically pressed into disks, and the disks were sintered at 800°C for 6 h. Sr-doped samples were prepared in the same

^{a)} Author to whom correspondence should be addressed; electronic mail: kueda1@rlem.titech.ac.jp

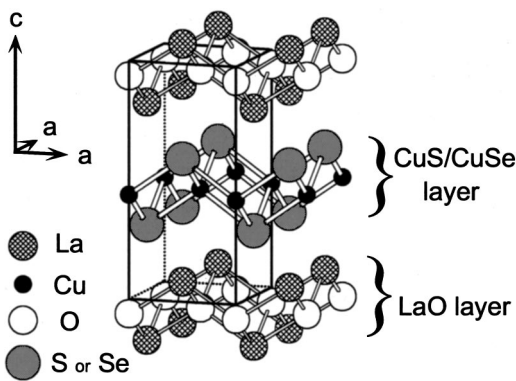


FIG. 1. Crystal structure of LaCuOS or LaCuOSe.

manner, and Sr ions were substituted for 2% of La ions as acceptors.

X-ray diffraction (XRD) patterns were measured to confirm a single phase in each sample. The Rietveld analysis was carried out to examine the crystal structure of the solid solutions and to refine crystal parameters such as lattice constants.¹³

The diffuse reflectance spectra of the powdered materials were measured at room temperature by using a spectrophotometer with an integrating sphere. The photoluminescence (PL) spectra of the disked samples were obtained at room temperature using a PL measurement system equipped with a charge coupled device detector. The fourth-harmonic wave (266 nm, $1 \text{ mJ cm}^{-2} \text{ pulse}^{-1}$) of a Nd:yttrium–aluminum–garnet laser (10 Hz, 15 ns pulse^{-1}) was used as excitation.

The electrical conductivities of the nondoped and Sr-doped samples were measured by the four-probe technique in the temperature range from room temperature to 20 K. Seebeck measurements were carried out on these samples at room temperature. In these electrical measurements, rectangular bars cut from the sintered disks were used as samples.

It was confirmed by XRD measurement that each sample was a single phase and a complete solid solution forms in the LaCuOS–LaCuOSe system. The lattice constants of $\text{LaCuOS}_{1-x}\text{Se}_x$ proportionally increased from 3.996 to 4.067 Å for a and from 8.517 to 8.798 Å for c with an increase in x from 0.0 to 1.0. The details of the crystal structure refinement of the solid solutions are reported elsewhere.¹⁴

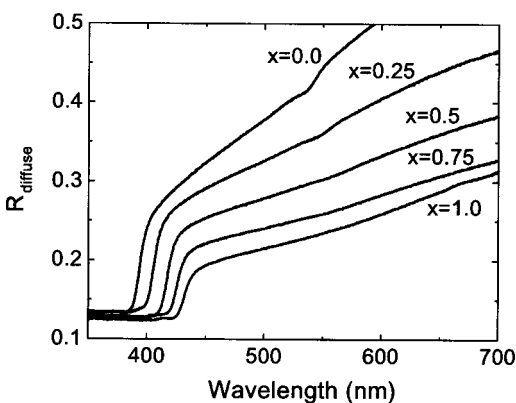


FIG. 2. Diffuse reflectance spectra of $\text{LaCuOS}_{1-x}\text{Se}_x$.

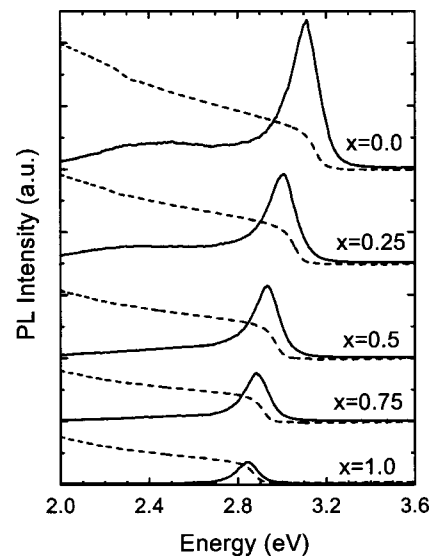


FIG. 3. PL spectra of $\text{LaCuOS}_{1-x}\text{Se}_x$. Diffuse reflectance spectra were superimposed with dashed lines.

The diffuse reflectance spectra of $\text{LaCuOS}_{1-x}\text{Se}_x$ are shown in Fig. 2. The color of the samples changed from brownish white to greenish gray as Se concentration increases. This change in color can be clearly seen in Fig. 2: The diffuse reflectance decreases and the position of the sharp reflectance drop shifts to longer wavelength with an increase in Se content. The sharp reflectance drop in Fig. 2 is regarded as the fundamental absorption edge of the samples, because diffuse reflectance is generally considered as optical transmittance through small crystals.

The PL spectra of $\text{LaCuOS}_{1-x}\text{Se}_x$ are shown in Fig. 3, along with their diffuse reflectance spectra. All samples showed relatively sharp emission peaks at the onset of the diffuse reflectance drop. The relative intensity of the band edge emission decreased with increasing x , probably due to the internal absorption.

The energy of the absorption edge was estimated in each sample by converting the diffuse reflectance into absorption by the Kubelka–Munk theory¹⁵ and drawing a $(\alpha h\nu)^2 - h\nu$ plot, where α , h , and ν denote absorption coefficient, Planck constant, and frequency, respectively. The energy gap estimated is plotted in Fig. 4 as a function of x . The peak-top

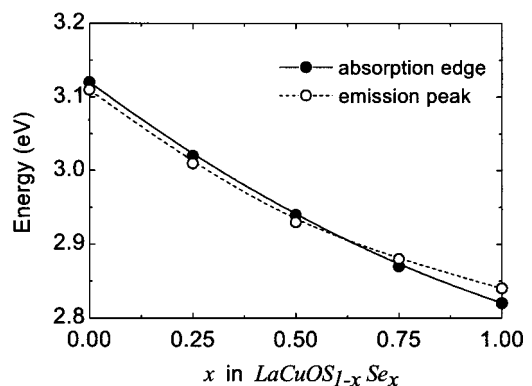


FIG. 4. The energies of absorption edge (solid circle) and emission peak (open circle) plotted as a function of x in $\text{LaCuOS}_{1-x}\text{Se}_x$.

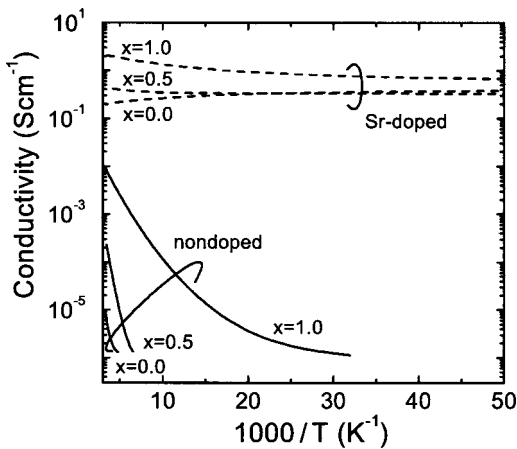


FIG. 5. Electrical conductivities of nondoped and Sr-doped $\text{LaCuOS}_{1-x}\text{Se}_x$ as a function of reciprocal temperature.

energy of the band edge emission in each PL spectrum is also plotted in Fig. 4. It is evident that the energies of the emission peaks are in good agreement with those of the absorption edges. This result demonstrates that the energy gap and the photon energy of the band edge emission can be controlled from 2.8 to 3.1 eV by chemical composition. In the case of LaCuOS , this band edge emission was assigned to room-temperature excitons in the previous study.⁹ Therefore, it is considered that the band edge emission observed in the $\text{LaCuOS}_{1-x}\text{Se}_x$ solid solutions also originates from room-temperature excitons.

Figure 5 shows the electrical conductivities of nondoped and Sr-doped $\text{LaCuOS}_{1-x}\text{Se}_x$ as a function of reciprocal temperature. Nondoped samples show semiconducting behavior, and the electrical conductivity increases with an increase in Se concentration. Carriers in the nondoped samples are considered to originate from Cu vacancies generated unintentionally during their preparation. Sr-doped samples show much higher electrical conductivity than the nondoped samples, and metallic or degenerate semiconducting behavior was observed. Seebeck coefficients of the nondoped samples ranged from +350 to +450 $\mu\text{V K}^{-1}$, while those of the Sr-doped samples ranged from +50 to +200 $\mu\text{V K}^{-1}$. The positive sign of these Seebeck coefficients in all samples

evidenced that the nondoped or Sr-doped $\text{LaCuOS}_{1-x}\text{Se}_x$ exhibits *p*-type electrical conduction. It was demonstrated from these results that Sr ions at La sites act effectively for hole generation as acceptors, and the *p*-type electrical conductivity of $\text{LaCuOS}_{1-x}\text{Se}_x$ can be controlled by Sr doping.

In conclusion, we controlled the band gap of $\text{LaCuOS}_{1-x}\text{Se}_x$ oxychalcogenides by the formation of a complete solid solution in the LaCuOS – LaCuOSe system. The energy gap of $\text{LaCuOS}_{1-x}\text{Se}_x$ varied from $E_g = 3.1$ eV to 2.8 eV with an increase in x from $x = 0.0$ to 1.0. The band edge emission was observed under UV excitation, and its peak energy agreed with the band gap energy in any composition of $\text{LaCuOS}_{1-x}\text{Se}_x$. The electrical conductivity of the solid solutions was controlled by Sr doping, and positive holes were responsible for the electrical conduction. The large energy gap, band edge emission, and *p*-type electrical conductivity suggest that $\text{LaCuOS}_{1-x}\text{Se}_x$ oxychalcogenides are promising materials for optoelectronic devices operating at short wavelengths, and their controllable band gap is expected to extend the optical applications of these materials.

- ¹S. Nakamura, T. Mukai, and M. Senoh, *Appl. Phys. Lett.* **64**, 1687 (1994).
- ²M. A. Haase, J. Qiu, J. M. DePuydt, and H. Cheng, *Appl. Phys. Lett.* **59**, 1272 (1991).
- ³H. Ohta, K. Kawamura, M. Orita, N. Sarukura, M. Hirano, and H. Hosono, *Electron. Lett.* **36**, 1 (2000); *Appl. Phys. Lett.* **77**, 475 (2000).
- ⁴S. Nakamura, M. Senoh, N. Iwasa, S. Nagahama, T. Yamada, and T. Mukai, *Jpn. J. Appl. Phys., Part 2* **34**, L1332 (1995).
- ⁵T. Mukai, H. Narimatsu, and S. Nakamura, *Jpn. J. Appl. Phys., Part 2* **37**, L479 (1998).
- ⁶Y. Sato, N. Takahashi, and S. Sato, *Jpn. J. Appl. Phys., Part 2* **35**, L838 (1996); **37**, L129 (1998).
- ⁷F. Hide, P. Kozodoy, S. P. DenBaars, and A. J. Heeger, *Appl. Phys. Lett.* **70**, 2664 (1997).
- ⁸K. Ueda, S. Inoue, S. Hirose, H. Kawazoe, and H. Hosono, *Appl. Phys. Lett.* **77**, 2701 (2000).
- ⁹K. Ueda, S. Inoue, H. Hosono, N. Sarukura, and H. Hirano, *Appl. Phys. Lett.* **78**, 2333 (2001).
- ¹⁰M. Palazzi, *Acad. Sci., Paris, C.R.* **292**, 789 (1981).
- ¹¹S. Inoue, K. Ueda, H. Hosono, and N. Hamada, *Phys. Rev. B* **64**, 245211 (2001).
- ¹²W. J. Zhu, Y. Z. Huang, C. Dong, and Z. X. Zhao, *Mater. Res. Bull.* **29**, 143 (1994).
- ¹³F. Izumi, in *The Rietveld Method*, edited by R. A. Young (Oxford University Press, London, 1993).
- ¹⁴K. Ueda and H. Hosono (unpublished).
- ¹⁵P. Kubelka and F. Munk, *Z. Tech. Phys. (Leipzig)* **12**, 593 (1931).